

Early-Stage Development of Human Induced Pluripotent Stem Cell-Derived Neurons

Yuki Ohara,¹ Noriko Koganezawa,¹ Hiroyuki Yamazaki,¹ Reiko T. Roppongi,¹ Kaoru Sato,² Yuko Sekino,² and Tomoaki Shirao¹*

¹Department of Neurobiology and Behavior, Gunma University Graduate School of Medicine, Maebashi, Gunma, Japan

²Division of Pharmacology, National Institute of Health Sciences, Tokyo, Japan

Recent advances in human induced pluripotent stem cells (hiPSCs) offer new possibilities for biomedical research and clinical applications. Differentiated neurons from hiPSCs are expected to be useful for developing novel methods of treatment for various neurological diseases. However, the detailed process of functional maturation of hiPSC-derived neurons (hiPS neurons) remains poorly understood. This study analyzes development of hiPS neurons, focusing specifically on early developmental stages through 48 hr after cell seeding; development was compared with that of primary cultured neurons derived from the rat hippocampus. At 5 hr after cell seeding, neurite formation occurs in a similar manner in both neuronal populations. However, very few neurons with axonal polarization were observed in the hiPS neurons even after 48 hr, indicating that hiPS neurons differentiate more slowly than rat neurons. We further investigated the elongation speed of axons and found that hiPS neuronal axons were slower. In addition, we characterized the growth cones. The localization patterns of skeletal proteins F-actin, microtubule, and drebrin were similar to those of rat neurons, and actin depolymerization by cytochalasin D induced similar changes in cytoskeletal distribution in the growth cones between hiPS neurons and rat neurons. These results indicate that, during the very early developmental stage, hiPS neurons develop comparably to rat hippocampal neurons with regard to axonal differentiation, but the growth of axons is slower. © 2015 The Authors. Journal of Neuroscience Research Published by Wiley Periodicals, Inc.

Key words: axonal development; growth cones; cytoskeletal proteins

Human induced pluripotent stem cell (hiPSC)-derived neuronal cells provide advantages for drug discovery, screening, and establishment of novel therapies (Yahata et al., 2011; Heilker et al., 2014). These cells have potential to detect human-specific side effects prior to clinical tests. Previous studies have utilized neurons differentiated from iPSCs that were developed from patients for therapeutic advancement in the treatment of Alzhei-

mer's disease, Parkinson's disease, and amyotrophic lateral sclerosis (Yagi et al., 2011; Egawa et al., 2012; Imaizumi et al., 2012; Chung et al., 2013). However, the detailed processes of functional maturation of hiPSC-derived neurons (hiPS neurons) are still largely unknown, and the mechanisms of development should be better understood before hiPS neurons are utilized as a tool for drug discovery and screening.

Neurons have the ability to form an axon and dendrites, which is important for information transfer in the central nervous system. Neuronal polarization goes through stereotypical changes leading to outgrowth of the axon and

SIGNIFICANCE:

Human induced pluripotent stem cell-derived neurons (hiPS neurons) offer new possibilities for biomedical research and clinical applications. Because humans have higher brain functions, differentiation of human neurons might have characteristics different from those of nonhuman neurons studied to date. This study focuses on early development of hiPS neurons and compares the development of cultured rat hippocampal neurons. Results indicate that morphological development of rat and human neurons before axonal polarization is similar. However, morphological development of axons in the hiPS neurons develops more slowly, showing especially slow elongation of the axon. This study also shows that the growth cone of hiPS neurons functions similarly to that of rat neurons.

N. Koganezawa and H. Yamazaki contributed equally to this work.

Contract grant sponsor: MHLW Health and Labor Sciences Research Grants for Research on Regulatory Science of Pharmaceuticals and Medical Devices; Contract grant sponsor: Japan Society for the Promotion of Science (JSPS); Contract grant numbers: 26860980; 26430063; 15K14344.

*Correspondence to: Tomoaki Shirao, MD, PhD, Professor and Chairman, Department of Neurobiology and Behavior, Gunma University Graduate School of Medicine, 3-39-22 Showa-machi, Maebashi, Gunma 371-8511, Japan. E-mail: tshirao@gunma-u.ac.jp

Received 25 May 2015; Revised 3 August 2015; Accepted 22 August 2015

Published online 8 September 2015 in Wiley Online Library (wileyonlinelibrary.com). DOI: 10.1002/jnr.23666

dendrites. Immature neurons have lamellipodia and filopodia that become multiple immature neurites at a later stage, and then one of the neurites grows rapidly to become an axon. This neuronal morphogenesis can be observed in cerebellar granule neurons, cortical neurons, and hippocampal neurons (Komuro et al., 2001; Hatanaka and Murakami, 2002; Noctor et al., 2004). Even under *in vitro* conditions, neurons are able to polarize to form an axon and multiple dendrites; this feature has been observed in rat hippocampal neurons (Dotti et al., 1988; Goslin and Banker, 1989; Craig and Banker, 1994) as well as in chick forebrain neurons (Heidemann et al., 2003).

This study investigates early developmental processes of hiPS neurons. We compared morphological features and localization of cytoskeletal proteins between rat neurons and hiPS neurons. Rat primary neurons cultured from the rat hippocampus were utilized because many studies have been performed and their development is well understood. iCell neurons (Cellular Dynamics International [CDI], Madison, WI) were utilized as the hiPS neurons. iCell neurons are a mixture of postmitotic neuronal subtypes composed primarily of γ -aminobutyric acidergic (GABAergic) and glutamatergic neurons. This composition is another reason for the comparison with rat hippocampal neurons, in which glutamate and GABA are the principal transmitters (Benson et al., 1994; Craig et al., 1994). Our results suggest that hiPS neurons develop similarly to rat neurons, although axonal polarization and growth are slower.

MATERIALS AND METHODS

Animal experiments were performed in accordance with the guidelines of the Animal Care and Experimentation Committee, Gunma University Showa Campus (Maebashi, Japan). Efforts were made to keep animal suffering to a minimum and to reduce the numbers of animals used.

Cell Cultures

Primary hippocampal cultures were prepared according to methods developed by Banker and Goslin (1998), with slight modifications (Takahashi et al., 2003).

Rat primary hippocampal cultures. Hippocampal neurons from embryonic day 18 Wistar rats (Charles River Laboratories Japan, Yokohama, Japan) were dissociated by trypsin treatment and triturated through a Pasteur pipette. The neurons were plated (5,000 cells/cm²) on coverslips (18 mm; Matsunami, Osaka, Japan), coated with poly-L-lysine (1 mg/ml), and incubated in minimum essential medium (MEM; Invitrogen, San Diego, CA) supplemented with 10% fetal bovine serum. Three hours later, the coverslips were transferred to a dish containing a glial monolayer sheet and were maintained in serum-free MEM with a B-27 supplement (Invitrogen).

hiPS neuron cultures. In this study, iCell neurons served as hiPS neurons. The cells were defrosted according to the protocol provided by the manufacturer. In total 7,000 cells/cm² were plated on coverslips (15 mm; Matsunami) coated with poly-L-lysine (1 mg/ml). The hiPS neurons were also incubated in MEM, and 3 hr later the coverslips were transferred to a glial sheet and maintained in B-27-supplied MEM. All cultures were

maintained at 35.8°C in an incubator with 5% CO₂ for 1–2 days *in vitro* (DIV).

Immunocytochemistry

Both rat neurons and hiPS neurons were fixed with 4% paraformaldehyde and 0.01% glutaraldehyde in 0.1 M phosphate-buffered saline (PBS) for 15 min at room temperature (RT). The cells were then washed twice with 0.1 M PBS and permeabilized with 0.1% Triton X-100 in PBS for 5 min. After being blocked with 3% bovine serum albumin in PBS (PBSA) for 60 min at RT, the cells were washed with PBS and incubated with primary antibodies in PBSA overnight at 4°C. The dilutions of primary antibodies were antidrebrin antibody (1:1; clone M2F6; hybridoma supernatant; RRID:AB_2532045; Shirao and Obata, 1986), anti- β -tubulin type III antibody (1:10,000; catalog No. G7121; RRID:AB_430874; Promega, Madison, WI), and antiphosphorylated neurofilament antibody (1:10,000; Sternberger Monoclonals, Baltimore, MD). F-actin was detected with rhodamine-conjugated phalloidin (Molecular Probes, Eugene, OR). Afterward, the cells were washed three times with PBS and incubated with appropriate species-specific secondary antibodies, fluorescein-conjugated anti-mouse IgG (MP Biomedicals, Aurora, OH), Cy5-conjugated anti-rabbit IgG (Chemicon, Temecula, CA), and Alexa Fluor 647 anti-rabbit IgG (Molecular Probes), in PBSA for 2 hr at RT. Finally, the cells were washed twice and mounted on slide glasses with PermaFluor mounting medium (Lab Vision, Fremont, CA) for microscopic evaluation. All neurons were analyzed with a conventional fluorescent microscope (Axio Imager 2; Zeiss, Jena, Germany) in MetaMorph microscopy automation and image analysis software (Meta Imaging V7.7; RRID:SciRes_000136; Molecular Devices, Sunnyvale, CA).

Antibody Characterization

See Table I for a list of all primary antibodies used. Antidrebrin antibody recognizes two bands of approximately 110 kDa molecular weight on Western blots of mouse brain. The upper band is drebrin A (adult isoform) and the lower is drebrin E (embryonic isoform). Only drebrin E is detected in the extract from drebrin A knockout mouse brain. No band is observed when drebrin null mutation mouse brain is used. Anti- β -tubulin type III antibody recognizes a single band of 50 kDa on Western blots. Antiphosphorylated neurofilament antibody recognizes bands of 160–200 kDa molecular weight on Western blots.

Time-Lapse Imaging

Prior to seeding, dissociated rat and hiPS neurons were transfected with pEGFP-C1 vector with Nucleofector (Lonza, Basel, Switzerland) according to the manufacturer's instructions. Both types of neurons were seeded on an Iwaki glass base dish (glass 12 mm; Asahi Glass, Tokyo, Japan) coated with poly-L-lysine (1 mg/ml) and maintained in MEM with B-27 supplement. These neurons were initially allowed to attach to the glass base and were then subsequently cocultured with glial cells seeded on coverslips (22 × 22 mm; Matsunami). The neurons were incubated in a confocal scanner box for live-cell imaging (Cell Voyager CV1000; Yokogawa Electric Corporation, Tokyo, Japan) at 35.8°C with 5% CO₂. Time-lapse images were acquired from 2

TABLE I. Primary Antibodies Used

Antigen	Description of immunogen	Source, host species, catalog/clone/lot No., RRID	Concentration used
Drebrin	Purified chicken drebrin E	Hybridoma supernatant, mouse monoclonal antibody, clone M2F6, RRID:AB_2532045	1:1
β -Tubulin type III	Synthetic peptide (EAQGPK) corresponding to the C-terminus of β III-tubulin	Promega, mouse monoclonal antibody, catalog No. G7121, clone 5G8, RRID:AB_430874	1:10,000 in PBSA
Phosphorylated neurofilament	Homogenized hypothalami recovered from Fischer 344 rats	Sternberger Monoclonals, mouse monoclonal antibody, catalog No. 837701, clone SMI-310	1:10,000 in PBSA

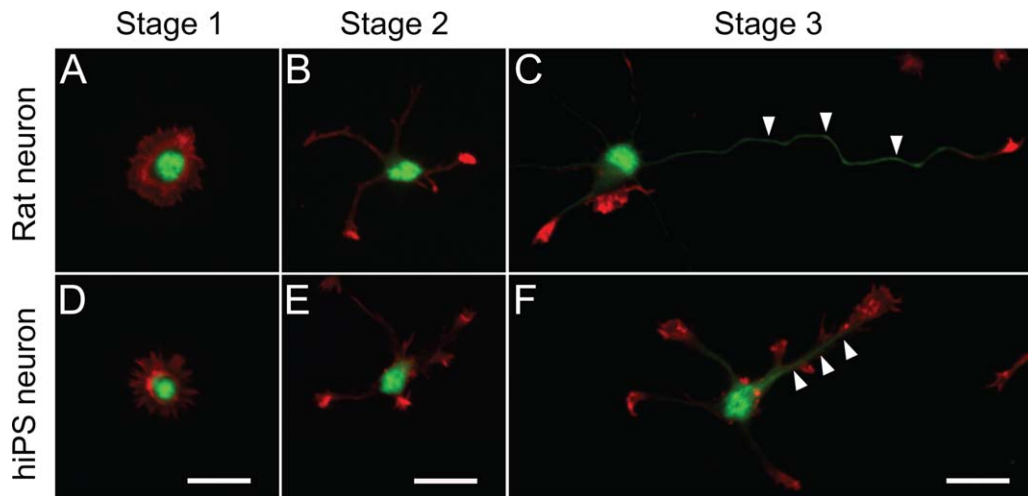


Fig. 1. Developmental classification of neurons. Rat hippocampal neurons and hiPS neurons were double labeled with antiphosphorylated neurofilament antibody (green, an axon marker) and rhodamine-conjugated phalloidin (red). Stage 1–3 neurons were observed in both rat neurons and hiPS neurons. **A,D**: Stage 1 cells at 5 hr after cell seeding. **B,E**: Stage 2 cells at 24 hr after cell seeding. **C,F**: Stage 3 cells at 48 hr after cell seeding. Axons are indicated with arrowheads. The axon of hiPS neurons was shorter compared with that of rat neurons. Scale bars = 20 μ m.

DIV cells every 10 min for 3 hr. In this time-lapse imaging experiment, cells with more than three neurites were observed as target cells, and the longest neurite was considered to be an axon. We used this morphological classification for identifying axons and dendrites because we were not able to use immunocytochemistry with antiphosphorylated neurofilament antibody on live cells. Although hiPS neurons sometimes had an axon that was not obviously longer than other neurites, our immunocytochemical analysis of fixed cells showed that the longest neurite was immunopositive for phosphorylated neurofilament. In addition, because the longer process has been used to represent the axon in rat neurons (Dotti et al., 1988), we used this morphological criterion in the time-lapse experiment to identify an axon.

Staging of Developing Neurons

The neurons were classified as stage 1 (Fig. 1A,D), stage 2 (Fig. 1B,E), or stage 3 (Fig. 1C,F) according to a classifica-

tion table suggested by Dotti et al. (1988), with minor modifications. After neurons had been labeled by rhodamine-conjugated phalloidin, neurites were defined as a process extending more than 10 μ m from the neuronal soma. An axon was defined as a neurite labeled by axonal markers, such as antiphosphorylated neurofilament antibody or antitau-1 antibody. We defined cell stages as stage 1, a cell without neurites; stage 2, a cell with some neurites that are not labeled by axonal markers, suggesting no axonal differentiation at this stage; and stage 3, a cell with an axon. Morphological analyses were performed in MetaMorph software.

Statistical Analysis

For multiple comparisons, the Steel-Dwass test was used, and the Welch's *t*-test or the Mann-Whitney U test was used for comparison between two groups. Statistical significance was set at $P < 0.01$.

RESULTS

Initial Maturation of Rat Neurons and hiPS Neurons

To evaluate maturation of developing neurons, we classified the neurons as stage 1, stage 2, or stage 3. We analyzed cells at 5, 24, and 48 hr after cell seeding and quantified the cell number at each stage to observe initial maturation. At each time point, the ratio of stage 1 cells was similar between rat neurons and hiPS neurons (Fig. 2Aa). At 5 hr after cell seeding, the majority of cells were still in stage 1. However, after 48 hr, the majority of cells had transformed into other stages. The shift to stage 2 was detectable at 5 hr after cell seeding in both neuronal populations, suggesting that development to stage 2 occurs in a similar manner (Fig. 2Ab). This was consistent with the fact that no significant differences in the ratio of stage 1 cells were observed (Fig. 2Aa). From 24 hr after cell seeding onward, however, the ratio of stage 2 cells was significantly greater in the hiPS neurons, suggesting that the shift to stage 3 occurred slowly in the hiPS neurons.

Differentiation Into Stage 3 Neurons

At 5 hr after cell seeding, it was difficult to observe stage 3 cells in the rat neurons and hiPS neurons. However, from 24 hr onward, there were some stage 3 cells in the rat neuronal population (Fig. 2Ac). After 48 hr, more than half of the rat neurons were at stage 3. However, less than 20% of hiPS neurons were at stage 3, even after 48 hr (Fig. 2Ac). In the rat neuronal population, stage 3 axons were fivefold (axon/dendrite = $5.51 \pm 0.41 \mu\text{m}$, $n = 56$) longer than other neurites (i.e., dendrites), whereas axonal length of hiPS neurons at stage 3 was only twofold (axon/dendrite = $2.11 \pm 0.17 \mu\text{m}$, $n = 33$) longer than the dendrites (Fig. 2Ba). There was no significant difference in dendrite length (rat, $30.68 \pm 1.69 \mu\text{m}$, $n = 75$; hiPS neuron, $27.46 \pm 1.90 \mu\text{m}$, $n = 33$; $P = 0.26$; Fig. 2Bb), whereas axonal length of hiPS neurons was significantly shorter than that of rat neurons (rat, $133.98 \pm 5.88 \mu\text{m}$, $n = 61$; hiPS neuron, $54.18 \pm 2.73 \mu\text{m}$, $n = 41$; $P < 0.01$; Fig. 2Bc). The hiPS neuronal axons and rat neuronal axons were immunostained with antiphosphorylated neurofilament antibody (stage 3; Fig. 1) and with antitau-1 antibody (data not shown). Collectively, these data suggest that axonal differentiation occurs in hiPS neurons as well, but axonal growth of hiPS neurons is slower than that of rat neurons, which could correlate with slower differentiation of hiPS neurons from stage 2 to stage 3.

We also quantified neurite number in stage 3 neurons and found that there was a significant difference between the average numbers of neurites (rat, 4.50 ± 0.15 , $n = 83$; hiPS neuron, 3.22 ± 0.18 , $n = 40$; $P < 0.01$; Fig. 2Bd). This result indicates that neuritogenesis was slower in hiPS neurons than in rat neurons, at least in their initial stages, which is consistent with a previous report (Harrill et al., 2011).

Axonal Growth of Rat Neurons and hiPS Neurons

Because axons were shorter in the hiPS neurons at DIV 2, we next investigated whether the shorter axon was due to slower growth or random growth directions. Both rat neurons and hiPS neurons were transfected with GFP, and time-lapse recordings were performed at DIV 2 for 3 hr with 10-min intervals. In this experiment, we used morphological classification for identifying axons and dendrites. The total growth after 3 hr was significantly greater in rat neuronal axons compared with hiPS neurons (rat, $33.57 \pm 4.07 \mu\text{m}$, $n = 17$; hiPS neuron, $5.12 \pm 1.58 \mu\text{m}$, $n = 16$; $P < 0.01$; Fig. 3A). The average growth was faster in rat axons than in hiPS neuron axons (rat, $11.84 \pm 1.95 \mu\text{m/hr}$; hiPS neuron, $1.80 \pm 1.42 \mu\text{m/hr}$; $P < 0.01$; Fig. 3B).

Axons do not always grow in one direction. In fact, they grow in various directions, and sometimes they even retract. Recordings were made every 10 min, and axonal length was compared frame by frame. If the axons were longer than in the former frame, we assumed that it was an elongation. Similarly, if the axons were shorter than in the former frame, we assumed that it was a retraction. We then compared elongation speed and retraction speed separately (Fig. 3C). We found that elongation of rat axons was significantly faster than that of hiPS neurons axons (rat, $29.32 \pm 1.75 \mu\text{m/hr}$; hiPS neuron, $18.78 \pm 1.51 \mu\text{m/hr}$; $P < 0.01$; Fig. 3Ca). However, we did not detect any significant differences in retraction speed between the two neuronal populations (rat, $-21.69 \pm 2.02 \mu\text{m/hr}$; hiPS neuron, $-15.53 \pm 1.16 \mu\text{m/hr}$; $P = 0.02$; Fig. 3Cb).

Next, we quantified the numbers of elongations or retractions within our recordings and calculated each ratio (Fig. 3D) to determine frequency of elongation or retraction. Because we performed time-lapse recordings for 3 hr with 10-min intervals, we had a total of 17 recording frames. In the rat neurons, elongation occurred more often than retraction (elongation, 65.7%; retraction, 34.3%; $P < 0.01$; Fig. 3Da), but both occurred equally in the hiPS neurons (elongation, 50.7%; retraction, 49.3%; $P = 0.67$; Fig. 3Db). These results indicate that axonal growth in the hiPS neurons was slower because of slower elongation and a lesser chance to elongate.

Cytoskeletons of the Growth Cones

Our results suggest that hiPS neurons differentiate normally, although elongation and differentiation are slower. We tested whether this was due to abnormalities in the growth cones. For this, we compared localization of cytoskeletal proteins, F-actin, β -tubulin (microtubules), and drebrin, between rat neurons and hiPS neurons. As shown in Figure 4A, in line with previous reports (Lin and Forscher, 1993; Mizui et al., 2009), the F-actin is distributed in the tips of growth cones, drebrin is localized in the middle, and β -tubulin is found in the proximal part. These patterns were similar in both rat neurons and hiPS neurons. Although our observation indicated that hiPS neurons had relatively small growth cones (Fig. 4A), there was no statistically significant difference in the average area of growth

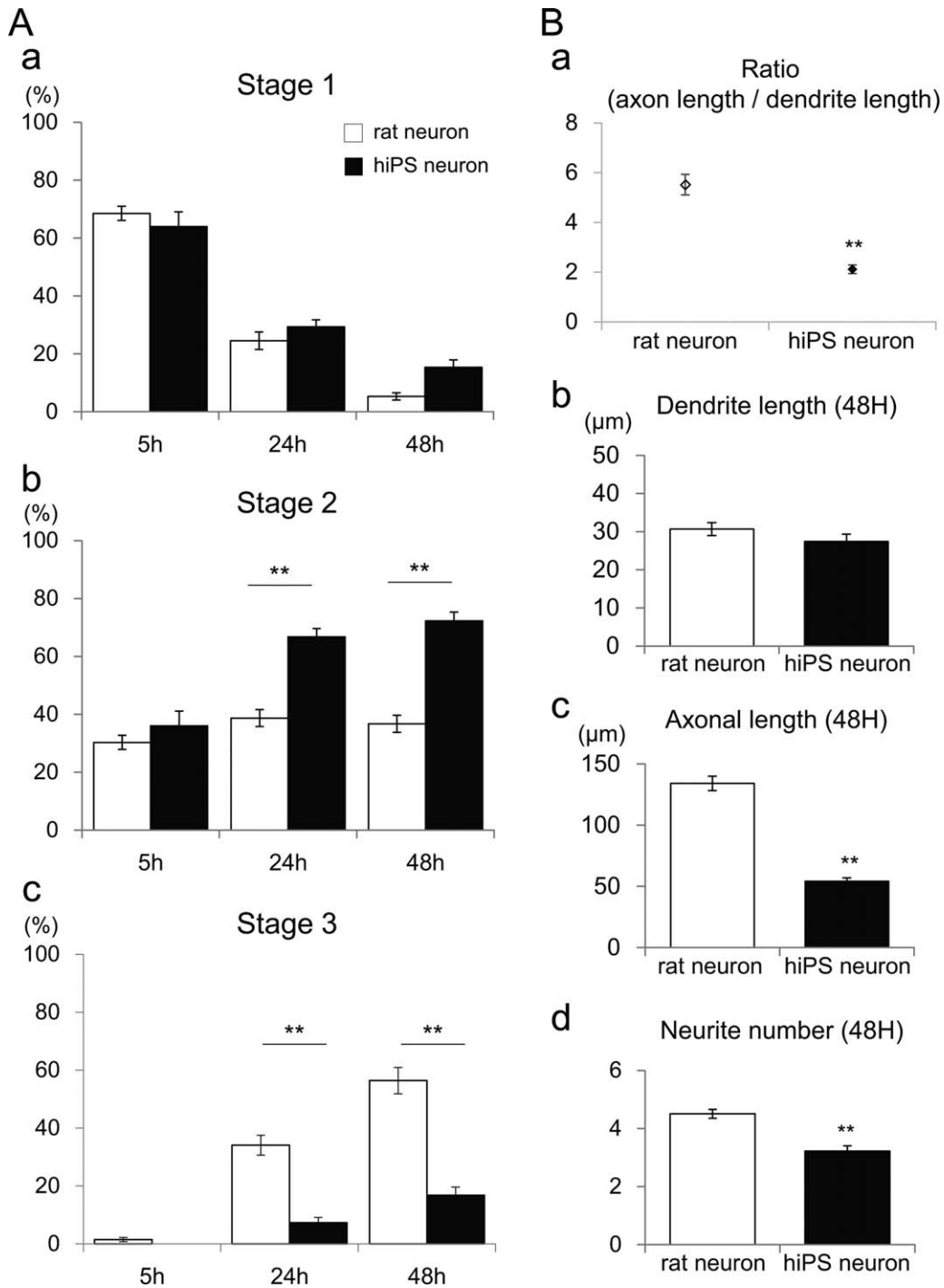


Fig. 2. Percentage of each stage and neurite length. **A**: Percentages of cells in each stage: stage 1 (**a**), stage 2 (**b**), stage 3 (**c**). Steel-Dwass test was used for statistical analysis, $n = 40$ per group. **B**: Analysis data of neurite length. Ratio of axonal length and dendrite length, rat neuron ($n = 56$) vs. hiPS neurons ($n = 33$), $P < 0.01$ (**a**). Dendritic length (rat,

$n = 75$; hiPS neuron, $n = 33$) and axonal length (rat, $n = 61$; hiPS neuron, $n = 41$) of both neurons at stage 3, 48 hr after cell seeding (**b,c**). Neurite number (rat, $n = 83$; hiPS neuron, $n = 40$) of both neurons at stage 3, 48 hr after cell seeding (**d**). Mann-Whitney U test was used in a,b,d, and Welch's t -test was used in c. $**P < 0.01$.

cones between rat neurons and hiPS neurons (rat, 61.03 ± 13.59 , $n = 60$; hiPS neuron, 45.62 ± 4.92 , $n = 40$; $P = 0.90$; Fig. 4B).

Cytochalasin D induces fragmentation and depolymerization of drebrin-free F-actin (Asada et al., 1994; Nair et al., 2008). We treated the DIV 2 neurons with $1 \mu\text{M}$

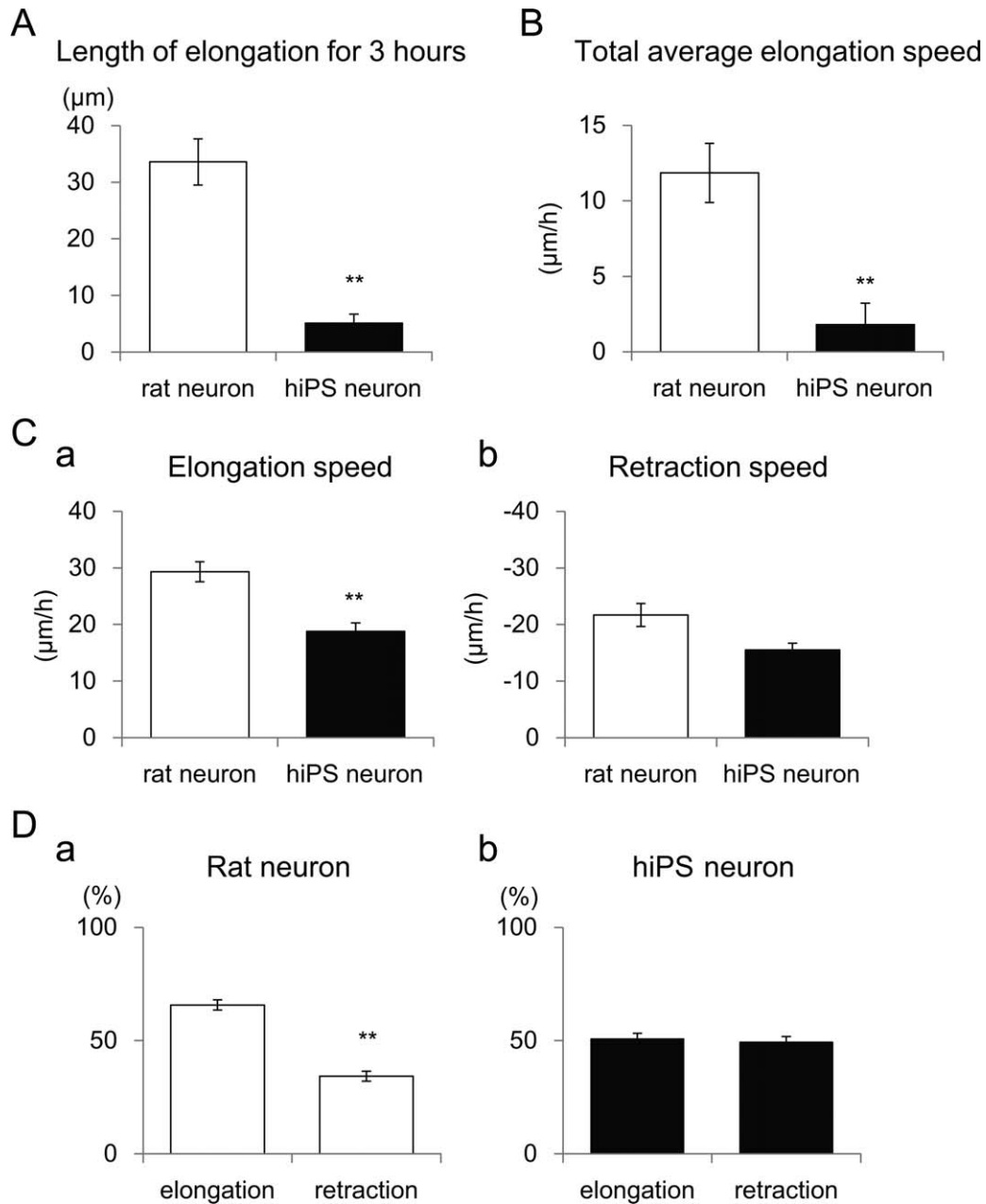


Fig. 3. Growth speed and growth direction of axons. **A**: Length of elongated axons for 3 hr measured by time-lapse recordings. **B**: Average elongation speed of axons, calculated by data from A. **C**: Elongation speed (**a**) and retraction speed (**b**), calculated from time-lapse recording data. **D**: Frequency of elongation or retraction (**a,b**). Welch's *t*-test was used in A, and Mann-Whitney U test was used in B–D; *n* = 17 (rat), *n* = 16 (hiPS neuron); ***P* < 0.01.

cytochalasin D (Sigma, St. Louis, MO) for 20 min and observed changes in localization of drebrin, F-actin, and β-tubulin. As shown in Figure 5, localization of drebrin and F-actin was changed to the tips of filopodia and lamellipodia following cytochalasin D treatment. As a result, microtubules extended into the edge of the growth cone in the rat neurons, which is in line with previously published results (Mizui et al., 2009). The reaction of these three pro-

teins was similar in the growth cones of the hiPS neurons. These data suggest that function of the growth cones is comparable between the rat neurons and the hiPS neurons.

DISCUSSION

We show that hiPS neurons and rat neurons develop similarly, but development of the hiPS neurons is

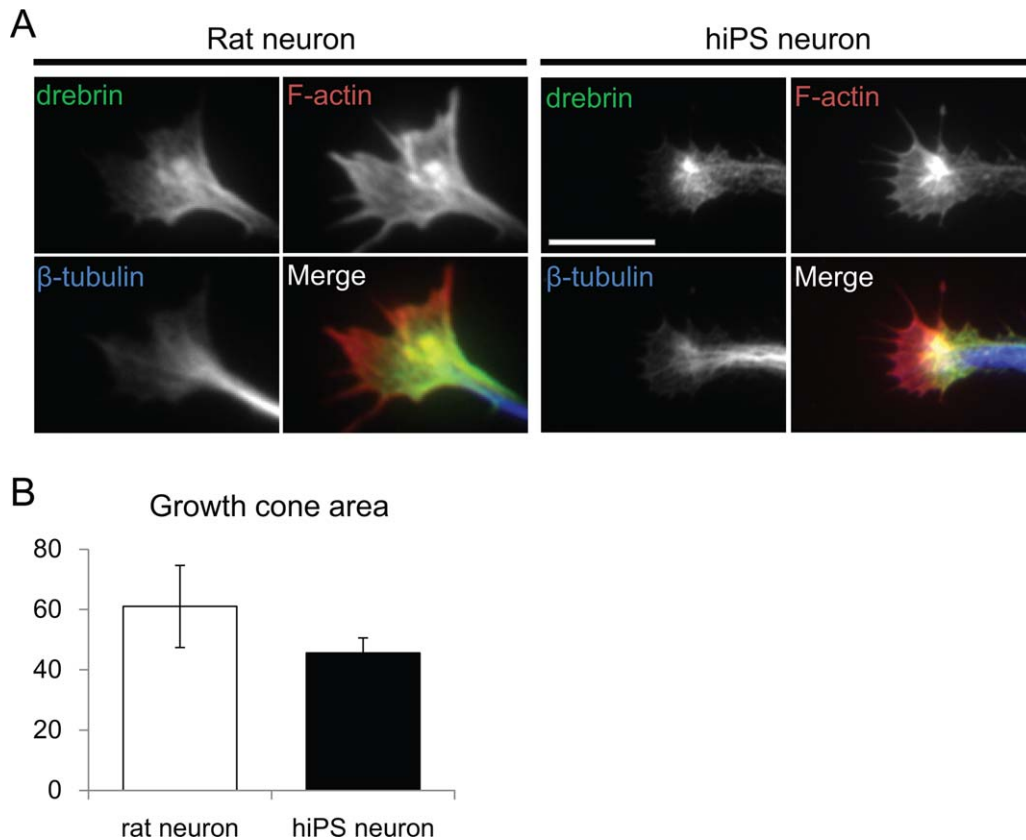


Fig. 4. **A**: Localization of skeletal proteins in the growth cones. F-actin (red) was localized to the peripheral domain in addition to the transitional zone. Microtubules (blue) were localized mainly at the central domain and also at the proximal part of the transitional zone. Drebrin (green) localization was mainly in the transitional zone. There

was no difference in the localization pattern of these proteins between rat neurons and hiPS neurons. **B**: Growth cone area of both neurons. There is no significant difference between areas of the two neuronal populations. Rat, $n = 60$; hiPS neuron, $n = 40$; Mann-Whitney U test; $P = 0.90$. Scale bar = 10 μm .

slower. In particular, axonal growth of the hiPS neurons is slower and the chance of elongation is lower. However, structural elements of the growth cone and their response to cytochalasin D are not different between rat and human neurons, suggesting that growth cone function is comparable between hiPS neurons and rat neurons.

Morphological Development Is Slightly Different Between Rat Neurons and hiPS Neurons

Morphological analysis demonstrates that the initial maturation of neurons from stage 1 to stage 2 occurs in a similar manner in both neuronal populations. Conversely, the shift from stage 2 to stage 3 occurs more slowly in hiPS neurons, suggesting that axonal polarization of the neurons is slower in hiPS neurons than in rat neurons. Furthermore, rat stage 3 neurons always have axons that are clearly longer than other neurites, whereas human stage 3 neurons sometimes have an axon that is not obviously longer than other neurites. These results suggest that axonal growth of the hiPS neurons is slower,

although those axons were immunopositive for axonal markers, such as phosphorylated neurofilament and tau-1. Moreover, we show that the neurite number of rat neurons is significantly greater than that of stage 3 hiPS neurons. This is consistent with a previous report in which primary rat cortical cultures and human embryonic stem cell-derived neuronal cultures were compared, showing that neurite length and neurite numbers are less in human neuronal cultures (Harrill et al., 2011). According to Harrill and colleagues (2011), this difference might be due to different protocols, fresh brain tissue vs. frozen stock, different species, or different sensitivity to components in the culture medium.

Average Axonal Growth Speed

The current results show that rat axons are more than fivefold longer than dendrites in stage 3, which is consistent with a previous report that the axonal growth speed of rat neurons is five- to tenfold greater than that of dendrites from stage 3 onward (Dotti et al., 1988). The hiPS neurons, however, have axons only twofold longer

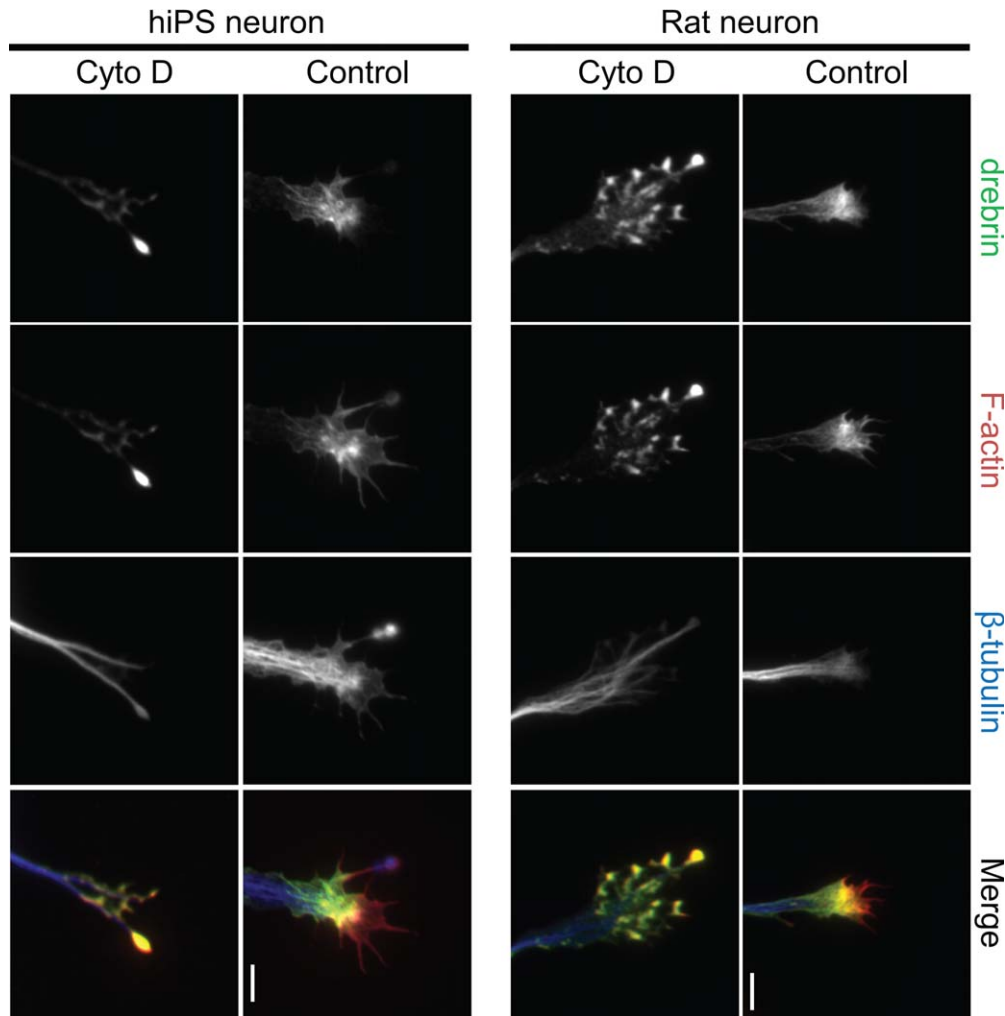


Fig. 5. Effect of cytochalasin D on growth cones. At 2 DIV, cultured rat neurons and hiPS neurons were treated with cytochalasin D (1 μ M) for 20 min and then stained for drebrin (green), F-actin (red), and β -tubulin (blue). Cytochalasin D treatments induced translocation of drebrin and F-actin from the transitional zone to the distal edge of the neurite growth cones in both neurons. Microtubules extended into the edge of the growth cone after the cytochalasin D treatments in both neurons. Cyto D, cytochalasin D. Scale bars = 5 μ m.

than the dendrites. In addition, the current data clearly show that axonal elongation of the rat neurons is faster than that of the hiPS neurons. A possible explanation is the difference in adhesion strength between rat neurons and hiPS neurons. However, the possibility of this is low because retraction speeds (which are different from elongation speeds) are similar between the two populations. Results from the present study also suggest that the increased speed of rat axonal growth is due to a greater frequency of elongation than retraction. In contrast, axons of hiPS neurons show no increase in elongation frequency. Therefore, another possible explanation is that hiPS neurons do not respond well to factors that induce elongation under our experimental conditions. We

observed a much longer axon in hiPS neurons at DIV 4 than at DIV 2 (data not shown), so we cannot exclude the possibility of greater axonal growth speed. Future studies are required to determine the mechanisms involved in promoting axonal growth of hiPS neurons and whether the axons grow faster in the later stage.

Function of the Growth Cones

Growth cones are important for guiding neurites during neuronal development. In neuronal growth cones, retrograde flow of actin is observed, and the flow is thought to play a role in axonal guidance and directed cell movement. Growth cones have three domains, a peripheral

domain, a central domain, and a transitional zone. The peripheral domain is composed of radial formations of unipolar F-actin bundles (Lewis and Bridgman, 1992), and the central domain is a microtubule-rich domain (Forscher and Smith, 1988). The actin arc lying between the peripheral and central domains is called the transitional zone, where F-actin bundles are decorated with drebrin E (Mizui et al., 2009). In the peripheral domain, F-actin bundles flow relatively quickly, whereas, in the transitional zone, actin arc structures move slowly (Schaefer et al., 2002). This slow movement might be due to binding of drebrin to F-actin (Geraldo and Gordon-Weeks, 2009; Mizui et al., 2009).

The current results show that F-actin, β -tubulin, and drebrin in the growth cone of hiPS neurons have localizations similar to those of rat neurons, as previously reported (Mizui et al., 2009). In addition, the average growth cone area is similar in both neurons, suggesting comparable growth cone functions in both neuronal populations. Furthermore, when we depolymerized F-actins that were not associated with drebrin, actin dynamics were inhibited, and the localizations of F-actin with drebrin intruded to the tip of filopodia similarly in both neuronal populations. This suggests that F-actin function is normal in hiPS neurons. Microtubule function also seems to be normal in hiPS neurons, given that we did not detect any differences in β -tubulin localization in either growth cone. Additionally, interactions between F-actins and microtubules are known to play important roles in growth cone steering (Rodriguez et al., 2003). In growth cones, drebrin interacts with end-binding protein 3 (EB3), a microtubule-binding protein (Geraldo et al., 2008). In both growth cones, microtubules enter the actin arc, where drebrin is present, but not the filopodia, where drebrin is absent. In contrast, in cytochalasin D-treated growth cones, both drebrin and microtubules enter the tip of filopodia in both neurons. Therefore, the interaction between drebrin and EB3 seems to be normal in both neuronal populations.

Comparison of Rat Neurons and hiPS Neurons

The hiPS neurons used in this study were provided by CDI. According to the information provided by CDI, these neurons are from the forebrain and are composed of GABAergic and glutamatergic neurons. Indeed, several studies that used iCell neurons showed functional AMPA, NMDA, and GABA_A receptors (Haythornthwaite et al., 2012; Dage et al., 2014). Because glutamate and GABA are the principal transmitters in rat hippocampal neurons (Benson et al., 1994; Craig et al., 1994), it can be assumed that these two neuronal populations contain similar cell types. Consequently, some studies made a comparison between rat neurons and human neurons (Harrill et al., 2011; Alhebshi et al., 2014). Because the hiPS neurons we used in this study have a forebrain identity, we assumed that we could compare rat neurons with the hiPS neurons. This assumption is also supported by a study showing that neurons initially develop in a similar manner, even when chick forebrain neurons and rat hip-

pocampal neurons were compared (Heidemann et al., 2003).

Our subjects were early-stage developmental hiPS neurons, making it difficult to discuss maturation of hiPS neurons compared with maturation of rat neurons at this point. However, it has been reported that hiPS neurons can be cultured long term and can form mature, functional neurons (Odawara et al., 2014). Odawara and colleagues (2014) also reported that hiPS neurons require a longer time to mature. Therefore, our findings of slow axonal maturation in hiPS neurons might be due to slower maturation of hiPS neurons over a longer period. Furthermore, to maintain the hiPS neurons for a longer time, coculture with rat astrocytes seems to be crucial, and physical contact with rat astrocytes is also important. Although our culture system used coculture with rat astrocytes, there was no physical contact. This could inhibit axonal growth. The optimal condition for hiPS neuronal cultures remains poorly understood. Therefore, further studies are required to define the ideal culture conditions, including culture medium constituents, sensitivity of neurons to chemical components, and physical contact with other cells for hiPS neuronal development.

To summarize the results from our study, morphological features during the early developmental stages (stages 1 and 2) are similar between rat and human neurons. However, from stage 3 onward, morphological development of the hiPS neurons is slower, suggesting that axonal differentiation of hiPS neurons occurs but at a slower rate. Because neurite formation of hiPS neurons until stage 2 seems to be similar to that of rat neurons, we might use the same evaluation methods for the neurite formation in assessment of developmental neurotoxicity of medicines. However, we must evaluate axonal polarization and development of hiPS neurons carefully because the standard manner of development has not yet been established.

CONFLICT OF INTEREST STATEMENT

The authors have no conflicts of interest to declare.

ROLE OF AUTHORS

All authors had full access to all data in the study and take responsibility for the integrity of the data and the accuracy of the data analysis. Study concept and design: YO, NK, HY, KS, YS, TS. Acquisition of data: YO, HY, RTR. Analysis and interpretation of data: YO, NK, HY, RTR. Preparation of the article: YO, NK, TS. Statistical analysis: NK, HY, RTR. Obtained funding: NK, HY, YS, TS. Study supervision: YS, TS.

REFERENCES

- Alhebshi AH, Odawara A, Gotoh M, Suzuki I. 2014. Thymoquinone protects cultured hippocampal and human induced pluripotent stem cells-derived neurons against alpha-synuclein-induced synapse damage. *Neurosci Lett* 570:126–131.
- Asada H, Uyemura K, Shirao T. 1994. Actin-binding protein, drebrin, accumulates in submembranous regions in parallel with neuronal differentiation. *J Neurosci Res* 38:149–159.

- Banker G, Goslin K. 1998. *Culturing nerve cells*. Cambridge, MA: MIT Press.
- Benson DL, Watkins FH, Steward O, Banker G. 1994. Characterization of GABAergic neurons in hippocampal cell cultures. *J Neurocytol* 23: 279–295.
- Chung CY, Khurana V, Auluck PK, Tardiff DF, Mazzulli JR, Soldner F, Baru V, Lou Y, Freyzon Y, Cho S, Mungenast AE, Muffat J, Mitalipova M, Pluth MD, Jui NT, Schule B, Lippard SJ, Tsai LH, Krainc D, Buchwald SL, Jaenisch R, Lindquist S. 2013. Identification and rescue of alpha-synuclein toxicity in Parkinson patient-derived neurons. *Science* 342:983–987.
- Craig AM, Banker G. 1994. Neuronal polarity. *Annu Rev Neurosci* 17: 267–310.
- Craig AM, Blackstone CD, Huganir RL, Banker G. 1994. Selective clustering of glutamate and gamma-aminobutyric acid receptors opposite terminals releasing the corresponding neurotransmitters. *Proc Natl Acad Sci U S A* 91:12373–12377.
- Dage JL, Colvin EM, Fouillet A, Langron E, Roell WC, Li J, Mathur SX, Mogg AJ, Schmitt MG, Felder CC, Merchant KM, Isaac J, Broad LM, Sher E, Ursu D. 2014. Pharmacological characterisation of ligand- and voltage-gated ion channels expressed in human iPSC-derived fore-brain neurons. *Psychopharmacology* 231:1105–1124.
- Dotti CG, Sullivan CA, Banker GA. 1988. The establishment of polarity by hippocampal neurons in culture. *J Neurosci* 8:1454–1468.
- Egawa N, Kitaoka S, Tsukita K, Naitoh M, Takahashi K, Yamamoto T, Adachi F, Kondo T, Okita K, Asaka I, Aoi T, Watanabe A, Yamada Y, Morizane A, Takahashi J, Ayaki T, Ito H, Yoshikawa K, Yamawaki S, Suzuki S, Watanabe D, Hioki H, Kaneko T, Makioka K, Okamoto K, Takuma H, Tamaoka A, Hasegawa K, Nonaka T, Hasegawa M, Kawata A, Yoshida M, Nakahata T, Takahashi R, Marchetto MC, Gage FH, Yamanaka S, Inoue H. 2012. Drug screening for ALS using patient-specific induced pluripotent stem cells. *Sci Transl Med* 4:145ra104.
- Forscher P, Smith SJ. 1988. Actions of cytochalasins on the organization of actin filaments and microtubules in a neuronal growth cone. *J Cell Biol* 107:1505–1516.
- Geraldo S, Gordon-Weeks PR. 2009. Cytoskeletal dynamics in growth-cone steering. *J Cell Sci* 122:3595–3604.
- Geraldo S, Khanzada UK, Parsons M, Chilton JK, Gordon-Weeks PR. 2008. Targeting of the F-actin-binding protein drebrin by the microtubule plus-tip protein EB3 is required for neurite outgrowth. *Nat Cell Biol* 10:1181–1189.
- Goslin K, Banker G. 1989. Experimental observations on the development of polarity by hippocampal neurons in culture. *J Cell Biol* 108: 1507–1516.
- Harrill JA, Freudenberg TM, Robinette BL, Mundy WR. 2011. Comparative sensitivity of human and rat neural cultures to chemical-induced inhibition of neurite outgrowth. *Toxicol Appl Pharmacol* 256: 268–280.
- Hatanaka Y, Murakami F. 2002. In vitro analysis of the origin, migratory behavior, and maturation of cortical pyramidal cells. *J Comp Neurol* 454:1–14.
- Haythornthwaite A, Stoelzle S, Hasler A, Kiss A, Mosbacher J, George M, Bruggemann A, Fertig N. 2012. Characterizing human ion channels in induced pluripotent stem cell-derived neurons. *J Biomol Screen* 17: 1264–1272.
- Heidemann SR, Reynolds M, Ngo K, Lamoureux P. 2003. The culture of chick forebrain neurons. *Methods Cell Biol* 71:51–65.
- Heilker R, Traub S, Reinhardt P, Scholer HR, Sternecker J. 2014. iPSC cell-derived neuronal cells for drug discovery. *Trends Pharmacol Sci* 35:510–519.
- Imaizumi Y, Okada Y, Akamatsu W, Koike M, Kuzumaki N, Hayakawa H, Nihira T, Kobayashi T, Ohyama M, Sato S, Takanashi M, Funayama M, Hirayama A, Soga T, Hishiki T, Suematsu M, Yagi T, Ito D, Kosakai A, Hayashi K, Shouji M, Nakanishi A, Suzuki N, Mizuno Y, Mizushima N, Amagai M, Uchiyama Y, Mochizuki H, Hattori N, Okano H. 2012. Mitochondrial dysfunction associated with increased oxidative stress and alpha-synuclein accumulation in PARK2 iPSC-derived neurons and postmortem brain tissue. *Mol Brain* 5:35.
- Komuro H, Yacubova E, Yacubova E, Rakic P. 2001. Mode and tempo of tangential cell migration in the cerebellar external granular layer. *J Neurosci* 21:527–540.
- Lewis AK, Bridgman PC. 1992. Nerve growth cone lamellipodia contain two populations of actin filaments that differ in organization and polarity. *J Cell Biol* 119:1219–1243.
- Lin CH, Forscher P. 1993. Cytoskeletal remodeling during growth cone-target interactions. *J Cell Biol* 121:1369–1383.
- Mizui T, Kojima N, Yamazaki H, Katayama M, Hanamura K, Shirao T. 2009. Drebrin E is involved in the regulation of axonal growth through actin-myosin interactions. *J Neurochem* 109:611–622.
- Nair UB, Joel PB, Wan Q, Lowey S, Rould MA, Trybus KM. 2008. Crystal structures of monomeric actin bound to cytochalasin D. *J Mol Biol* 384:848–864.
- Noctor SC, Martinez-Cerdeno V, Ivic L, Kriegstein AR. 2004. Cortical neurons arise in symmetric and asymmetric division zones and migrate through specific phases. *Nat Neurosci* 7:136–144.
- Odawara A, Saitoh Y, Alhebshi AH, Gotoh M, Suzuki I. 2014. Long-term electrophysiological activity and pharmacological response of a human induced pluripotent stem cell-derived neuron and astrocyte coculture. *Biochem Biophys Res Commun* 443:1176–1181.
- Rodriguez OC, Schaefer AW, Mandato CA, Forscher P, Bement WM, Waterman-Storer CM. 2003. Conserved microtubule-actin interactions in cell movement and morphogenesis. *Nat Cell Biol* 5:599–609.
- Schaefer AW, Kabir N, Forscher P. 2002. Filopodia and actin arcs guide the assembly and transport of two populations of microtubules with unique dynamic parameters in neuronal growth cones. *J Cell Biol* 158: 139–152.
- Shirao T, Obata K. 1986. Immunohistochemical homology of 3 developmentally regulated brain proteins and their developmental change in neuronal distribution. *Brain Res* 394:233–244.
- Takahashi H, Sekino Y, Tanaka S, Mizui T, Kishi S, Shirao T. 2003. Drebrin-dependent actin clustering in dendritic filopodia governs synaptic targeting of postsynaptic density-95 and dendritic spine morphogenesis. *J Neurosci* 23:6586–6595.
- Yagi T, Ito D, Okada Y, Akamatsu W, Nihei Y, Yoshizaki T, Yamanaka S, Okano H, Suzuki N. 2011. Modeling familial Alzheimer's disease with induced pluripotent stem cells. *Hum Mol Genet* 20:4530–4539.
- Yahata N, Asai M, Kitaoka S, Takahashi K, Asaka I, Hioki H, Kaneko T, Maruyama K, Saido TC, Nakahata T, Asada T, Yamanaka S, Iwata N, Inoue H. 2011. Anti-A β drug screening platform using human iPSC cell-derived neurons for the treatment of Alzheimer's disease. *PLoS One* 6:e25788.